Inorganic Chemistry

Article

pubs.acs.org/IC

Mono- and Binuclear Copper(I) Complexes of Thionucleotide Analogues and Their Catalytic Activity on the Synthesis of Dihydrofurans

D. C. Charalampou,[†] N. Kourkoumelis,[‡] S. Karanestora,[§] L. P. Hadjiarapoglou,[§] V. Dokorou,[⊥] S. Skoulika,[⊥] A. Owczarzak,[∥] M. Kubicki,[∥] and S. K. Hadjikakou*[,†]

[†]Section of Inorganic and Analytical Chemistry, Department of Chemistry, [‡]Medical Physics Laboratory, Medical School, [§]Section of Organic Chemistry, Department of Chemistry, and [⊥]X-ray Unit, Department of Chemistry, University of Ioannina, 45110 Ioannina, Greece

[∥]Faculty of Chemistry, Adam Mickiewicz University, Grunwaldzka 6, 60-780 Poznan, Poland

Supporting Information

ABSTRACT: The reaction of copper(I) halides with 2-thiouracil (TUC), 6-methyl-2-thiouacil (MTUC), and 4-methyl-2-mercaptopyrimidine (MPMTH) in the presence of triphenylphosphine (tpp) in a 1:1:2 molar ratio results in a mixed-ligand copper(I) complex with the formulas $[Cu_2(tpp)_4(TUC)Cl]$ (**1**), $[Cu_2(tpp)_4(MTUC)Cl]$ (**2**), $[Cu(tpp)_2(MPMTH)Cl]\cdot{}^1/_2CH_3OH$ (**3**), $[Cu(tpp)_2(MTUC)Br]$ (**4**), and $[Cu(tpp)_2(MTUC)I]\cdot{}^1/_2CH_3CN$ (**5**). The complexes have been characterized by FT-IR, ^{1}H NMR, and UV−vis spectroscopic techniques and single-crystal X-ray crystallography. Complexes **1** and **2** are binuclear copper(I) complexes. Two phosphorus atoms from tpp ligands are coordinated to the copper(I) ions, forming two units that are linked to each other by a deprotonated TUC or MTUC chelating ligand through a sulfur bridge. A linear Cu−S−Cu moiety is formed. The tetrahedral geometry around the metal centers is completed by the nitrogen-donor atom from the TUC or MTUC ligand for the one unit, while for the other one, it is completed by the chloride anion. Two phosphorus atoms from two tpp ligands, one sulfur atom from MPMTH or MTUC ligand, and one halide anion (Cl, Br, and I) form a tetrahedron around the copper ion in **3**−**5** and two polymorphic forms of **4** (**4a** and **4b**). In all of the complexes, either mono- or binuclear intramolecular O−H···X hydrogen bonds enhance the stability of the structures. On the other hand, in almost all cases of mononuclear complexes (with the exception of a symmetry-independent molecule in **4a**), intermolecular NH···O hydrogen-bonding interactions lead to dimerization. Complexes **1**−**5** were studied for their catalytic activity for the intermolecular cycloaddition of iodonium ylides toward dihydrofuran formation by HPLC, ^{1}H NMR, and LC-HRMS spectroscopic techniques. The results show that the geometry and halogen and ligand types have a strong effect on the catalytic properties of the complexes. The highest yield of dihydrofurans was obtained when "linear" complexes **1** and **2** were used as the catalysts. The activity of the metal complexes on the copper(I)-catalyzed and uncatalyzed intramolecular cycloaddition of iodonium ylide is rationalized through electronic structure calculation methods, and the results are compared with the experimental ones.

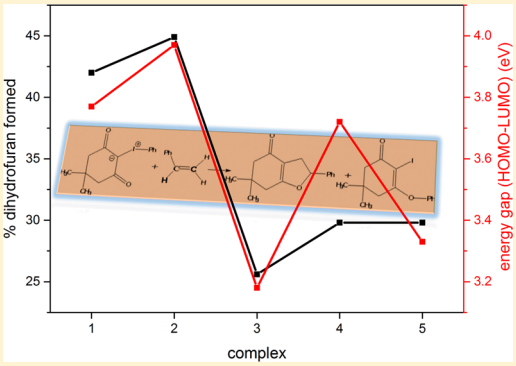

INTRODUCTION

Dihydrofurans and their derivatives have demonstrated a wide range of applications in modern pharmaceutical research.[1] Dihydrofurans are used as pharmaceutical agents or basic precursors in the synthesis of important drugs such as antiallergic, antimicrobial, or anticancer drugs.[2−4] Recently, they have been studied as anti-HIV[3,4] agents and β-amyloid aggregation inhibitors[1a,5] related to Alzheimer's disease. Therefore, the development of novel synthetic routes for dihydrofurans is of great chemical and pharmaceutical interest. The reaction of phenyliodonium dimedonate with unsaturated reagents has been investigated since the late 1980s,[6] and the reaction of phenyliodonium dimedonate with styrene under photochemical activation leads to the formation of dihydrofurans (reaction 1). When the reaction mixture is heated without irradiation, only iodoether is obtained[6] (reaction 2). However, when copper acetate is present as the catalyst, the mixture of products contains dihydrofuran and iodoether (reaction 3).

The mechanism of the intramolecular rearrangement of phenyliodonium ylides of hydroxyquinones was investigated theoretically.[7] It has been proposed that phenyliodonium ylides of hydroxyquinones can easily undergo intramolecular rearrangements associated with phenyl-group migration or ketene formation.[7] Phenyl-group migration is favorable thermodynamically when the reaction mixture is heated. Our research

Received: March 29, 2014

   dx.doi.org/10.1021/ic500727z | *Inorg. Chem.* XXXX, XXX, XXX−XXX

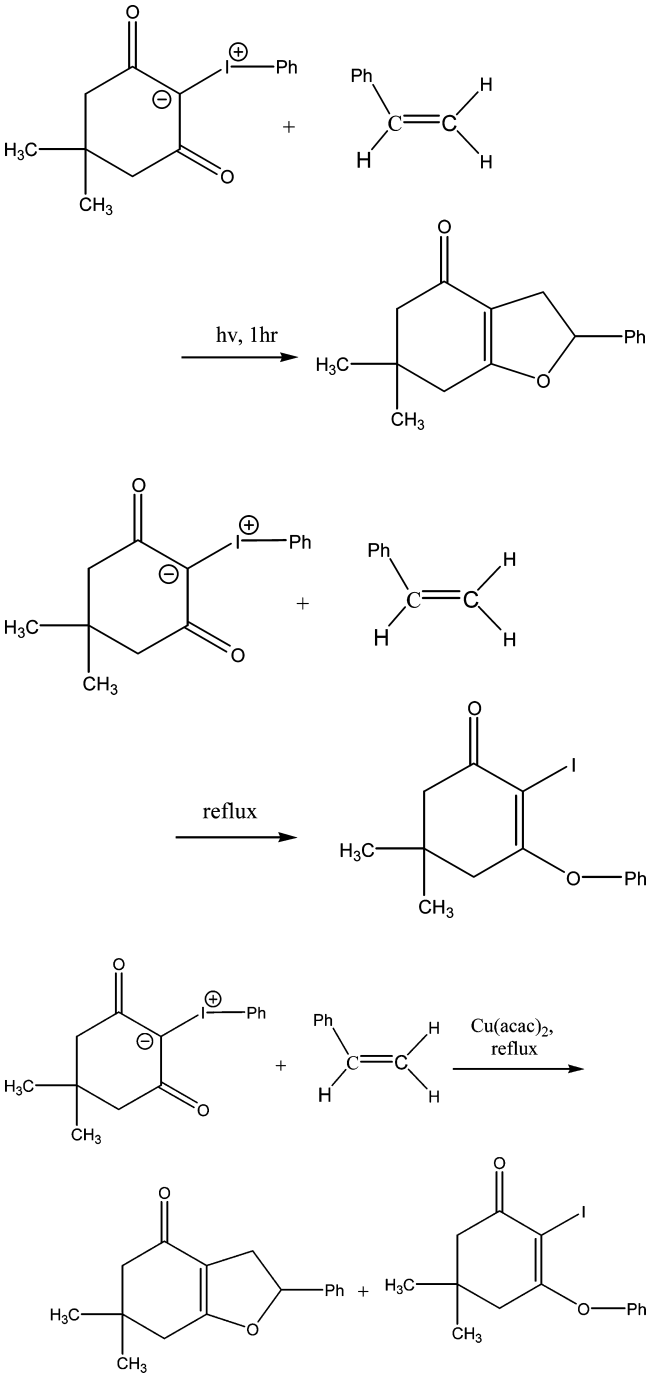

group has recently shown that, during dihydrofuran formation from the reaction of phenyliodonium dimedonate with styrene, IPh dissociation occurred with a simultaneous attack of styrene to the cyclohexyl ion via a Friedel–Crafts mechanism (reactions 1 and 3).[8]

The influence of the catalyst type on the product formation is still an intriguing question for the development of new catalysts for the synthesis of new dihydrofurans. Several catalysts and catalytic systems, such as $[Rh(CO)_2acac]$,[9a] $[Rh_2(OAc)_4]$,[9b] $[Pd(OAc)_2]/[CuI]$,[9c] $[Pd(PPh_3)4]$,[9d] $[Cu(OTf)_2]$,[9e] $[Cu(phen)(PPh_3)]NO_3$,[9e] $[Ph_3PAuNTf_2]$,[9f] [MePosAuCl]/$AgNTf_2$,[9f] etc., have been used, resulting in various yields with different time and cost effectiveness. Copper-based catalysts have shown great potential regarding their efficiency.[9e]

We have recently demonstrated that copper(I) complexes $[CuI(ptu)_2]$(toluene) (ptu = 6-*n*-propyl-2-thiouracil), $[CuI(tpp)_2(ptu)]$ (tpp = triphenylphosphine), and $[CuI(tptp)_2(ptu)]$ (tptp = tri-*p*-tolylphosphine), $[(tpSb)_2Cu(\mu_2\text{-}I)_2Cu(tpSb)_2]$ (tbSb = triphenylstilbine), $[(tpp)Cu(\mu_2\text{-}I)_2Cu(tpp)_2]$, $[(tpp)Cu(\mu_2\text{-}Cl)_2Cu(tpp)_2]$, and $[CuCl(tpp)_3\cdot(CH_3CN)]$[8] catalyze the formation of dihydrofurans in addition to copper(II) acetate,[6] indicating that the mechanism might not be a redox process. Similarly, these copper(I) complexes were found to exhibit higher catalytic activity than the corresponding one of the gold(I) complex [AuCl(tpp)].[8] Both monomeric and dimeric copper(I) complexes with trigonal and tetrahedral geometry around the metal center exhibit strong catalytic activity. In this case, iodo-containing complexes have shown better activity than the ones with chlorine.

Our work aims at the design and development of new efficient catalyst for dihydrofuran formation. Here we report the synthesis of new copper(I) halide complexes with the formulas $[Cu_2(tpp)_4(TUC)Cl]$ (**1**), $[Cu_2(tpp)_4(MTUC)Cl]$ (**2**), $[Cu(tpp)_2(MPMTH)Cl]\cdot{}^1/_2CH_3OH$ (**3**). $[Cu(tpp)_2(MTUC)Br]$ (**4**), and $[Cu(tpp)_2(MTUC)I]\cdot{}^1/_2CH_3CN$ (**5**), where TUC = 2-thiouacil, MTUC = 6-methyl-2-thiouracil, MPMTH = 4-methyl-2-mercaptopyrimidine, and tpp = triphenylphosphine (Scheme 1). The complexes have been characterized by Fourier transform infrared (FT-IR), ^{1}H NMR, and UV–vis spectroscopic techniques and single-crystal X-ray crystallography. The stability of the complexes in solution has been confirmed by conductivity measurements and ^{1}H NMR spectroscopy. Mercaptopyrimidine derivatives (TUC, MTUC, and MPMTH) have been chosen as a result of their biological applications because they are nucleotide analogues acting as ligands with sulfur-donor atoms. The highly lipophilic tpp ligand has been chosen because of its solubility in organic solvents and because of the induced stabilization of the copper(I) oxidation state of the metal ion. The agile Cu–P bond, on the other hand, promotes the catalytic activities of the metal ion. The catalytic activity of complexes **1**–**5** on the intermolecular cycloaddition of iodonium ylides toward dihydrofuran formation was studied. The corresponding catalytic effect of copper(II) ions in the form of $[Cu(acac)_2]^{2+}$ is already reported.[6] To ascertain whether this catalytic activity is a redox process or not, copper(I)

Scheme 1

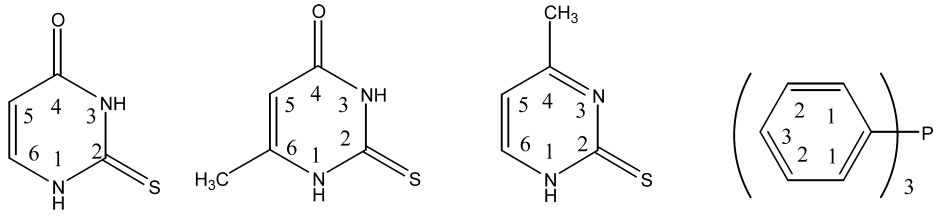

dx.doi.org/10.1021/ic500727z | Inorg. Chem. XXXX, XXX, XXX–XXX

Scheme 2

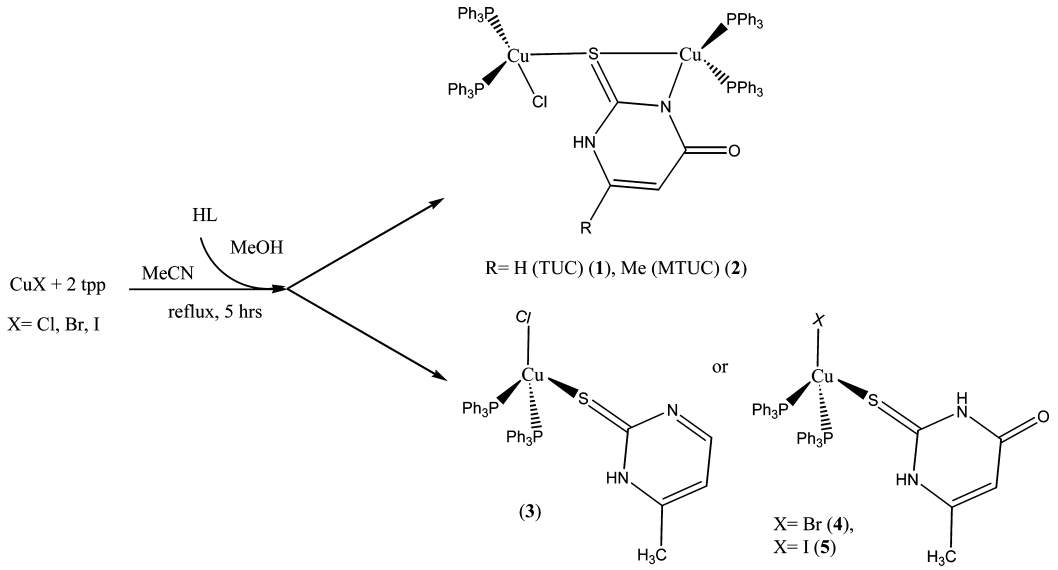

iodide complexes **1**–**5** were synthesized. The structural diversity of **1**–**5** allows the structure–activity relationship study of these compounds on the dihydrofuran formation reaction. Because both irradiation and catalysts promote the formation of dihydrofurans, the photocatalytic process is also investigated here. Thereby, new, more efficient catalysts can be developed from this work.

RESULTS AND DISCUSSION

General Aspects. Complexes **1**–**5** have been prepared by reacting copper(I) halides with TUC, MTUC, and MPMTH in the presence of tpp in a 1:1:2 molar ratio in a 1:1 methanol/acetonitrile solution (Scheme 2). Crystals of complexes **1**–**5** have been grown by slow evaporation of the solutions, which remain after filtration of the reaction solutions. The crystals of the complexes are air-stable when they remain in darkness at room temperature. The formulas of the complexes were deduced from their spectroscopic data and single-crystal X-ray crystallography. Complexes **1**–**5** are soluble in toluene, $CHCl_3$, CH_2Cl_2, MeCN, CH_3OH, and acetone.

The stability of complexes **1**–**5** was tested by ^1H NMR in a $CDCl_3$ solution and by conductivity measurements in MeCN solutions. No changes were observed between the initial ^1H NMR spectrum and the corresponding spectra when measured after 24, 48, and 72 h and 1 week (Figures S1–S5 in the Supporting Information, SI). No ionic species were formed; the molar conductance (Λm) values of the complexes in a MeCN solution (10^{-3} M) were for **1** 13.4 (0 h), 21.6 (24 h), 25.6 (48 h), 30.9 (72 h), and 35.6 (1 week) Ω^{-1} cm^2 mol^{-1}, for **2** 24.8 (0 h), 30.4 (24 h), 33.7 (48 h), 39.1 (72 h), and 42.8 (1 week) Ω^{-1} cm^2 mol^{-1}, for **3** 13.3 (0 h), 22.7 (24 h), 27.6 (48 h), 34.6 (72 h), and 40.8 (1 week) Ω^{-1} cm^2 mol^{-1}, for **4** 25.1 (0 h), 30.3 (24 h), 32.9 (48 h), 37.8 (72 h), and 40.9 (1 week) Ω^{-1} cm^2 mol^{-1}, and for **5** 39.2 (0 h), 44.8 (24 h), 45.5 (48 h), 52.1 (72 h), and 57.2 (1 week) Ω^{-1} cm^2 mol^{-1}. The experiments were carried out at 11.4–24.2 °C. Because the molar conductance of acetonitrile solutions of the complexes at 10^{-3} M for 1:1 type electrolytes lies in the range of 120–160 Ω^{-1} cm^2 mol^{-1} (220–330 Ω^{-1} cm^2 mol^{-1} for 2:1 electrolytes), the values measured for **1**–**5** show nonconducting behavior, confirming their stability in acetonitrile.[9g]

Vibrational Spectroscopy. The IR spectra of the compounds were recorded in the range 4000–300 cm^{-1}. Apart from the existence of strong phosphine bands, the usual four "thioamide bands" confirm the presence of heterocyclic thione ligands; the characteristic NH stretching vibrations are observed in the 3050–3160 cm^{-1} region. The lack of ν(SH) bands at 2500–2600 cm^{-1} signifies the exclusive S-coordination mode of the thione ligands. The IR spectra of complexes **1**–**5** (Figures S6–S10 in the SI) show distinct vibrational bands at 1532 and 1434 cm^{-1} (**1**), 1535 and 1360 cm^{-1} (**2**), 1561 and 1435 cm^{-1} (**3**), 1493, 1391, 1480, and 1391 cm^{-1} (**4**), and 1480 and 1385 cm^{-1} (**5**), respectively, which can be assigned to ν(CN) vibrations (thioamide I and II bands), and at 1170 and 920 cm^{-1} (**1**), 844 and 606 cm^{-1} (**2**), 1306 and 795 cm^{-1} (**3**), 823 and 455 cm^{-1} (**4**), and 841 and 456 cm^{-1} (**5**), respectively, which are attributed to the ν(CS) vibrations (thioamide III and IV bands). The corresponding thioamide bands of the free ligands are observed at 1565, 1421, 1210, and 809 cm^{-1} for TUC, at 1520, 1413, 871, and 598 cm^{-1} for MTUC, and at 1587, 1410, 1270, and 835 cm^{-1} for MPMTH, respectively (Figures S11–S14 in the SI).[10]

Crystal and Molecular Structures of Complexes 1–5. The structures of complexes **1**–**5** were determined by X-ray diffraction. Molecular diagrams of complexes **1**–**5** are shown in Figures 1–6, and selected bond distances and angles are given in Table 1.

Complexes **1** and **2** are dimers of quite an unusual composition. Despite the different ligands (TUC in **1** and MTUC in **2**), their structures are quite similar. The structure of **1** is described in detail herein, while the appropriate numerical values for **2** are included in square brackets. One of the copper ions (Cu1) is tetrahedrally coordinated with two phosphine atoms (from PPh_3 groups), one chlorine, and the sulfur atom from the TUC ligand. The tetrahedron is slightly distorted, probably because of the repulsion between the tpp groups (the P–Cu–P angle is 126.62(5)° [127.23(4)°]; the same feature is observed throughout the whole series; cf. Table 1). The second copper, Cu2, is only weakly bound to the sulfur atom (Cu–S 2.8873(16) Å [2.9692(12) Å]); on the contrary, it is coordinated by the N2 atom from TUC. Technically (not taking into account the probable secondary Cu···S contact), this copper ion is 3-coordinated, in a trigonal fashion. The sum of the X–Cu–Y bond angles with three coordinating atoms

dx.doi.org/10.1021/ic500727z | Inorg. Chem. XXXX, XXX, XXX–XXX

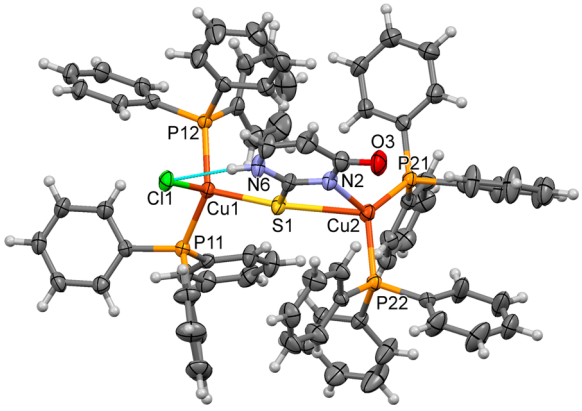

Figure 1. Perspective view of complex **1**. Ellipsoids are drawn at the 50% probability level, and hydrogen atoms are shown as spheres of arbitrary radii. The dashed line denotes an intramolecular hydrogen bond; note that both short and long S−Cu interactions are shown (cf. the text).

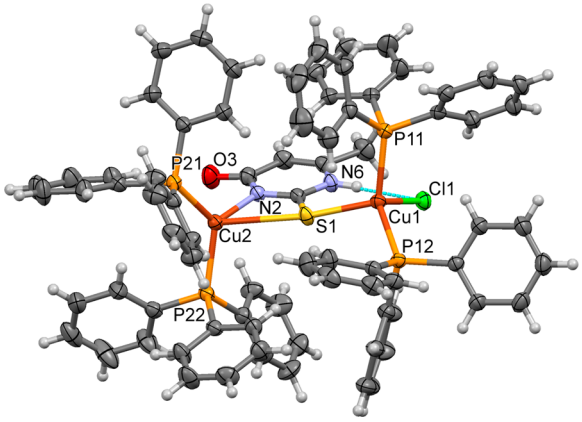

Figure 2. Perspective view of complex **2**. Ellipsoids are drawn at the 50% probability level, and hydrogen atoms are shown as spheres of arbitrary radii. The dashed line denotes an intramolecular hydrogen bond; note that both short and long S−Cu interactions are shown (cf. the text).

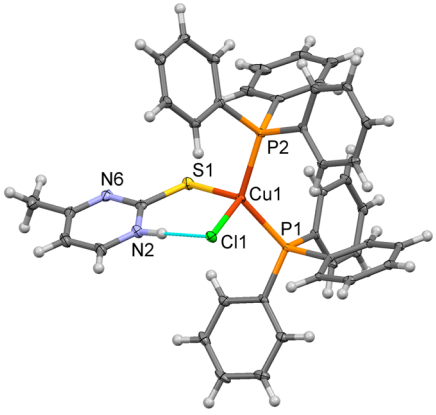

Figure 3. Perspective view of complex **3**. Ellipsoids are drawn at the 50% probability level, and hydrogen atoms are shown as spheres of arbitrary radii. The dashed line denotes an intramolecular hydrogen bond.

(P21, P22, and N2) is 358.3° [359.3°], and copper is only slightly, by 0.1481(15) Å [0.1036(9) Å], pushed out of the P−P−N plane. TUC and MTUC are deprotonated, and they

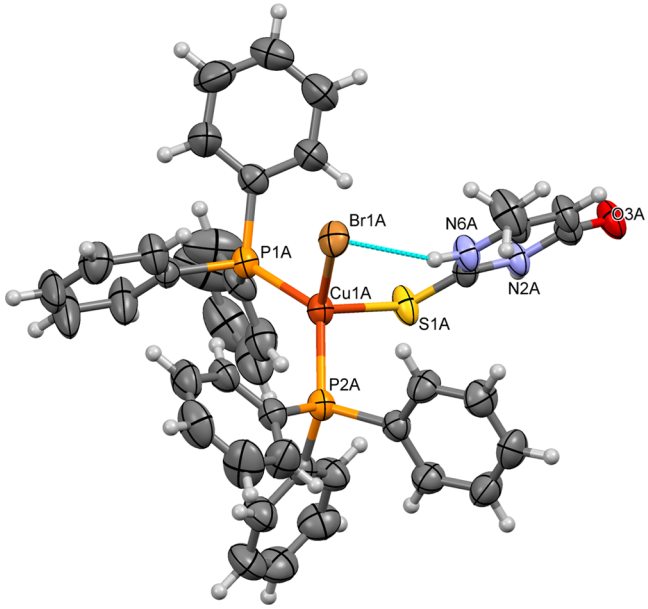

Figure 4. Perspective view of one of the symmetry-independent molecules of complex **4a**. Ellipsoids are drawn at the 50% probability level, and hydrogen atoms are shown as spheres of arbitrary radii. The dashed line denotes an intramolecular hydrogen bond.

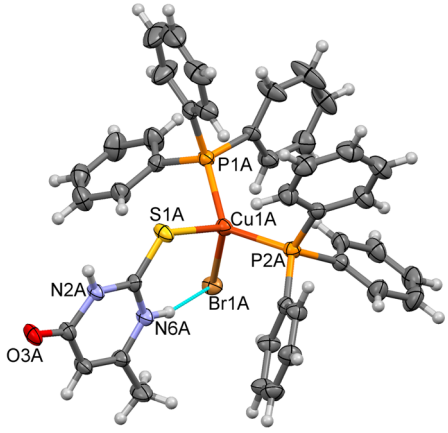

Figure 5. Perspective view of one of the symmetry-independent molecules of complex **4b**. Ellipsoids are drawn at the 50% probability level, and hydrogen atoms are shown as spheres of arbitrary radii. The dashed line denotes an intramolecular hydrogen bond.

are coordinated in their monoanionic form. Two phosphorus atoms, from the two tpp ligands, have bond lengths equivalent with each copper(I) cation (Table 1). The bond-length values are within the average of Cu−P (av. 2.290 Å), Cu−Cl (2.375 Å) and Cu−S (2.387 Å) bond lengths reported in the literature[11−15] for mixed-ligand copper(I) chloride complexes with phosphines and thiones. Therefore, the TUC and MTUC ligands are chelating the Cu2 metal centers. The Cu−S···Cu angles are almost linear [173.02(6)° (**1**) and 172.99° (**2**)]. Two different stereoisomers can be obtained because of the orientation of the keto and/or methyl groups of TUC and MTUC (Scheme 2). Thus, on the basis of the nitrogen atom that is deprotonated (N2; Figures 1 and 2), only one isomer was isolated for **1** and **2**. The isomers were further stabilized by intramolecular hydrogen-bonding interactions between the H[N] (N6; Figures 1 and 2) and chlorine atoms. Table 2 contains the hydrogen-bond data for all compounds. To the best

dx.doi.org/10.1021/ic500727z | Inorg. Chem. XXXX, XXX, XXX−XXX

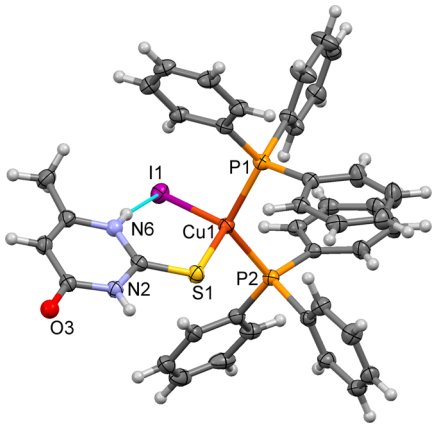

Figure 6. Perspective view of complex **3**. Ellipsoids are drawn at the 50% probability level, and hydrogen atoms are shown as spheres of arbitrary radii. The dashed line denotes an intramolecular hydrogen bond.

of our knowledge, this linear assembly of the two copper units observed in **1** or **2** is unique, and these are the first structures of mixed-ligand copper(I) complexes with such a configuration.

Complexes **3**–**5** are monomers. Complex **4** was isolated in two polymorphic forms (**4a** and **4b**), both crystallizing into two symmetry-independent molecules (A and B) in the asymmetric part of the unit cell (Table 1). The copper centers in complexes **3**–**5** (**3**, **4a**, **4b**, and **5**) are 4-coordinated (according to **1** and **2**) by two phosphorus atoms from the tpp ligands, one sulfur atom from MPMT (**3**) and MTUC (**4** and **5**), and one halogen atom [Cl (**3**), Br (**4a** and **4b**), and I (**5**)]. The geometry is slightly distorted tetrahedral; the distortion is, as in the case of **1** and **2**, mainly caused by the arrangement of the bulky tpp ligands (cf. Table 1). In general, the Cu–P or Cu–X bond lengths are in agreement with those found in similar structures. The average Cu–Cl bond distance is 2.375 Å, the corresponding one of Cu–Br is 2.501 Å, and that of Cu–I is 2.675 Å (Table 2).[8,14,15] The average Cu–P bond distance is 2.290 Å in copper chloride

Table 1. Selected Bond Distances (Å) and Angles (deg) of Complexes 1–5

	1 (X = Cl)	**2** (X = Cl)	**3** (X = Cl)	**4a(A)** (X = Br)	**4a(B)**	**4b(A)**	**4b(B)**	**5**
Cu1–P11	2.2683(13)	2.2980(14)	2.2761(9)	2.281(4)	2.291(4)	2.2758(11)	2.2768(12)	2.2772(7)
Cu1–P12	2.2959(16)	2.2730(9)	2.2825(9)	2.277(4)	2.271(4)	2.2797(11)	2.2977(11)	2.2824(7)
Cu1–X1	2.3877(14)	2.3902(10)	2.3539(9)	2.4892(19)	2.5109(19)	2.5049(7)	2.5152(7)	2.6572(4)
Cu1–S1	2.3867(15)	2.3773(11)	2.3571(11)	2.398(4)	2.365(4)	2.3907(12)	2.4005(12)	2.3897(7)
Cu2–N2	1.985(4)	1.980(2)						
Cu2–P21	2.2322(14)	2.2378(10)						
Cu2–P22	2.2664(15)	2.2621(14)						
Cu2···S1	2.8873(16)	2.9692(12)						
C1–S1	1.696(5)	1.718(3)	1.691(3)	1.679(12)	1.662(14)	1.672(3)	1.674(3)	1.677(2)
C3–O3	1.224(5)	1.230(4)		1.226(14)	1.222(15)	1.229(4)	1.223(4)	1.227(3)
P11–Cu1–P12	126.62(5)	127.23(4)	123.78(3)	114.93(14)	122.91(16)	129.32(4)	115.24(4)	119.65(2)
C1–N2–C3	121.7(4)	121.2(2)	122.2(3)	124.0(11)	124.6(11)	125.4(3)	125.8(3)	124.0(2)
C1–N6–C5	121.5(4)	121.8(2)	118.7(3)	125.5(10)	126.2(12)	124.1(3)	124.1(3)	126.0(2)

Table 2. Hydrogen-Bond Data (Å and deg)[a]

			Complex **1**			
N6	H6	Cl1		2.24	3.094(4)	175
			Complex **2**			
N6	H6	Cl1		2.28	3.137(3)	176
			Complex **3**			
N2	H2	Cl1	0.98	2.06	3.036(3)	177
O1A	H1A	N6	0.90	2.04	2.900(16)	159
			Complex **4a**			
N2A	H2AA	Br1A	0.88	2.53	3.275(10)	144
N2B	H2BA	Br1B	0.88	2.35	3.223(10)	169
N6A	H6A	$O3A^{I}$	0.88	1.96	2.829(13)	170
N6B	H6B	$O3B^{II}$	0.88	2.03	2.889(15)	164
			Complex **4b**			
N6A	H6A	Br1A	0.86	2.45	3.264(3)	158
N6B	H6B	Br1B	0.86	2.42	3.213(3)	154
N2A	H2A	$O3A^{III}$	0.86	1.95	2.808(4)	176
N2B	H2B	$O3B^{IV}$	0.86	1.94	2.796(4)	171
			Complex **5**			
N2	H2	I1	0.84(3)	2.74(3)	3.551(2)	164(3)
N6	H6	$O3^{V}$	0.83(2)	2.01(2)	2.834(3)	171(3)

[a]Symmetry codes: I, $-x, -y, -z$; II, $1-x, y, {}^{1}/_{2}-z$; III, $1-x, 1-y, 1-z$; IV, $2-x, 1-y, -z$; V, $x, 1+y, 1+z$.

dx.doi.org/10.1021/ic500727z | Inorg. Chem. XXXX, XXX, XXX–XXX

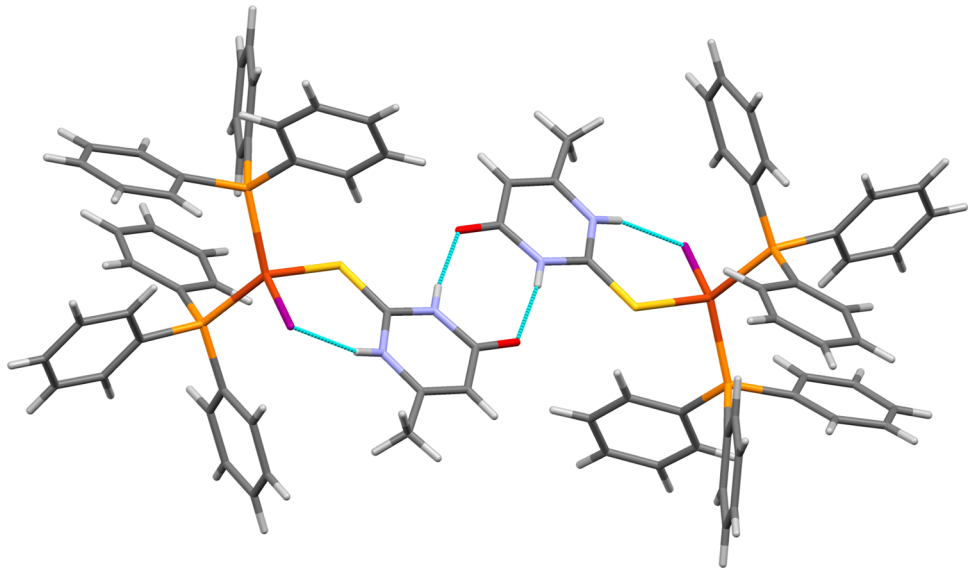

Figure 7. Example of the hydrogen-bonded dimer present in the structures **3**−**5**. The figure shows the case of **5**. Dashed lines show both intra- and intermolecular hydrogen bonds.

complexes, 2.283 Å in copper bromide complexes, and 2.289 Å in copper iodide ones, while the average Cu−S is 2.387 Å in copper chloride complexes, 2.362 Å in copper bromide complexes, and 2.366 Å in copper iodide ones (Table 1).[8,11−15] It is worth mentioning that the Cu−P and Cu−S bond distances are independent of the nature of the halogen ligand present in the complexes. The bond angles around the copper centers in the cases of **3**−**5** varied between 98° and 124°, with the higher distortion detected for the P−Cu−P angle due to the valence-shell electron-pair repulsions.

Two different stereoisomers can be obtained because of the orientation of the keto and/or methyl groups of MPMTH and MTUC in the cases of **3**−**5** (Scheme 1). However, the arrangement of the methyl group (Scheme 1) indicates that only the one isomer has been isolated for **3**−**5**. Intermolecular hydrogen-bonding interactions between the H[N] and halogen (Scheme 2) lead to the formation of only one isomer (Table 2). In **3**, the solvent (methanol) molecule acts as a hydrogen-bond donor for the N6 atom of the MPMTH molecule. The difference between protonated (N2) and unprotonated nitrogen atoms is also visible in the values of the C−N−C bond angles. In the structures of **4a**, **4b**, and **5**, intermolecular N−H···O3 hydrogen bonds form supramolecular structures (Table 2). For molecules (i) A of **4a**, (ii) both molecules of **4b**, and (iii) molecule **5**, these hydrogen bonds create centrosymmetric dimers (C_i internal symmetry; see Figure 7 as an example). On the other hand, molecules B from the structure **4a** make hydrogen-bonded dimers, but the molecules are related by a 2-fold axis along *y* featuring C_2 symmetry for the dimer. This diverse supramolecular organization shows that, in fact, these forms are polymorphs of different crystal architecture.

Solution Studies. *^{1}H NMR Spectroscopy.* The ^{1}H NMR spectra of complexes **1**−**5** (Figures S15−S19 in the SI) show multiple resonance signals, which are attributed to $H_{aromatic}$ of tpp at 7.35−7.30 (**1**), 7.45−7.31 (**2**), 7.49−7.41 (**3**), 7.46−7.37 (**4**), and 7.46−7.33 (**5**) ppm for $H^2_{arom\_tpp}$ and $H^3_{arom\_tpp}$ (Scheme 1) and at 7.24−7.21 (**1**), 7.25−7.22 (**2**), 7.24−7.21 (**3**), 7.24−7.21 (**4**), and 7.26−7.23 (**5**) ppm for $H^1_{arom\_tpp}$ (Scheme 1). The resonance signal at the 7.12−7.09 ppm doublet (**1**) is due to $H(C^6)_{pyr\_ring}$ (Scheme 1) of the pyrimidine ring. The resonance signals at the 5.77 ppm doublet (**1**), 5.63 ppm singlet (**2**), 6.54 ppm doublet (**3**), 5.62 ppm singlet (**4**), and 5.64 ppm singlet (**5**) are due to $H(C^5)_{pyr\_ring}$ (Scheme 1) of the pyrimidine ring (Figures S15−S19 in the SI). The singlet signals at 2.12 (**2**), 2.43 (**3**), 2.11 (**4**), and 2.18 (**5**) ppm are assigned to H_3C of the methyl substituent. The signals at 1.27 (**2**), 1.27 (**3**), 1.27 (**4**), and 1.27 (**5**) ppm are assigned to $H(N^1)$ or $H(N^3)$ of the amide groups of the pyrimidine ring. In the cases of complexes **3** and **4**, the signals at 3.49 and 3.50 ppm are attributed to H(O) of the cocrystallized solvent molecule (MeOH). The singlet signals at 1.56 ppm are assigned to the water molecules of the solvent ($CDCl_3$). The proton ratio $[H(N):H(C^5)_{pyr\_ring}:H^1_{arom\_tpp}:H^{2,3}_{arom\_tpp}]$ remains unchanged in solution, indicating retention of the structure in chloroform (Figures S15−S19 in the SI).

Catalysis. The catalytic activity of complexes **1**−**5** was tested upon reaction of phenyliodonium dimedonate with styrene (phenylethylene) for the formation of dihydrofuran (reaction 4). Styrene also serves as the solvent medium. The reaction takes place at 110 °C for 45 and 120 s under aerobic conditions. The dihydrofuran and iodoether yields were detected by high-performance liquid chromatography (HPLC; Table 3). The retention times of the products were detected by standard samples of pure dihydrofuran and iodoether and confirmed by

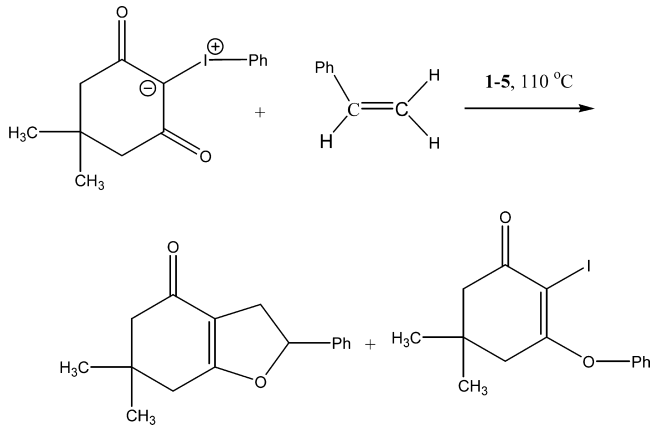

dx.doi.org/10.1021/ic500727z | Inorg. Chem. XXXX, XXX, XXX−XXX

Table 3. Catalytic Activity of 1−5 upon the Reaction of Phenyliodonium Dimedonate with Styrene for the Formation of Dihydrofuran and Iodoether

catalyst	amount of catalyst (mg)	reaction time (s)	dihydrofuran[a] (area %)	iodoether[b] (area %)	ratio B/I
control		45	11.3	48.5	0.2
1	0.5	45	35.9	17.2	2.1
1	0.5	120	42.0	9.1	4.6
1	1.0	45	37.8	6.7	5.6
1	1.0	120	38.1	8.5	4.5
1	4.0	45	38.6	8.2	4.7
1	4.0	120	36.4	7.3	5.0
2	0.5	45	44.9	9.6	4.7
2	0.5	120	40.6	18.6	2.4
2	1.0	45	43.1	13.7	3.1
2	1.0	120	37.4	7.6	4.9
2	4.0	45	38.5	10.6	3.6
2	4.0	120	34.9	11.2	3.1
3	0.5	45	23.7	33.8	0.7
3	1.0	45	24.3	34.3	0.7
3	4.0	45	25.6	33.7	0.8
4	0.5	45	24.2	63.2	0.4
4	0.5	120	24.8	62.9	0.4
4	1.0	45	24.6	62.6	0.4
4	1.0	120	26.5	61.2	0.4
4	4.0	45	29.4	59.9	0.5
4	4.0	120	29.8	58.9	0.5
5	0.5	45	10.6	69.6	0.2
5	0.5	120	9.9	55.1	0.2
5	1.0	45	23.9	64.1	0.4
5	1.0	120	29.8	59.5	0.5
5	4.0	45	18.9	67.0	0.3
5	4.0	120	25.6	61.7	0.4

[a]The retention time is 10.5 ± 0.5 min at λ_{max} = 280 nm. [b]The retention time is 16.4 ± 0.4 min at λ_{max} = 280 nm.

liquid chromatography−electrospray ionization mass spectrometry (LC−ESI-MS) spectra (Figure S20 in the SI). The products of the reaction are also analyzed by ^{1}H NMR spectroscopy and LC−ESI-MS.

The results show that the binuclear copper(I) complexes (**1** and **2**) exhibit higher catalytic activity [higher dihydrofuran yields of 42% (**1**) and 44.9% (**2**)] than the mononuclear complexes [**3**−**5**; higher dihydrofuran yields of up to 26% (**3**), 30% (**4**), and 30% (**5**)]. The order of the catalytic activity is **2** > **1** > **4** = **5**> **3**. Generally, **1**−**5** show better catalytic activity than the previous mixed-ligand monomeric or dimeric copper(I) complexes [CuI(ptu)$_2$](toluene), [CuI(tpp)$_2$(ptu)], [CuI(tptp)$_2$(ptu)], [(tpSb)$_2$Cu(μ_2-I)$_2$Cu(tpSb)$_2$], [(tpp)Cu(μ_2-I)$_2$Cu(tpp)$_2$], [(tpp)Cu(μ_2-Cl)$_2$Cu(tpp)$_2$], and [CuCl(tpp)$_3$·(CH$_3$CN)][8] used. The higher dihydrofuran yield is 27.3% when [CuI(ptu)$_2$](toluene) is used as the catalyst, 32.7% with the use of [CuI(tpp)$_2$(ptu)], 33% with [CuI(tptp)$_2$(ptu)], 41.3% with [(tpp)Cu(μ_2-I)$_2$Cu(tpp)$_2$], 26.6% with [(tpp)Cu(μ_2-I)$_2$Cu(tpp)$_2$], 25.6% with [(tpp)Cu(μ_2-Cl)$_2$Cu(tpp)$_2$], and 26.2% with [CuCl(tpp)$_3$·(CH$_3$CN)][8] (Table 4). Both the monomeric [CuI(tptp)$_2$(ptu)] and dimeric [(tpSb)$_2$Cu(μ_2-I)$_2$Cu(tpSb)$_2$] copper(I) complexes with tetrahedral geometry around the metal centers were found to exhibit strong catalytic activity.[8] These activities were lower than the corresponding ones measured for the binuclear complexes **1** and **2**, indicating that the nuclearity of the complex has a strong effect on its catalytic activity along with the type of ligand bound to the metallic center.

Table 4. Dihydrofuran Obtained from Phenyliodonium Dimedonate and Styrene under the Catalytic Activity of Copper(I) Complexes as an Ingredient (%) of the Product Mixture

complex	%	ref
2	44.9	*a*
1	42.0	*a*
[(tpSb)$_2$Cu(μ_2-I)$_2$Cu(tpSb)$_2$]	41.3	8
[CuI(tptp)$_2$(ptu)]	33.0	8
[CuI(tpp)$_2$(ptu)]	32.7	8
4	30.0	*a*
5	30.0	*a*
[CuI(ptu)$_2$](toluene)	27.3	8
[(tpp)Cu(μ_2-I)$_2$Cu(tpp)$_2$]	26.6	8
[CuCl(tpp)$_3$·(CH$_3$CN)]	26.2	8
3	26.0	*a*
[(tpp)Cu(μ_2-Cl)$_2$Cu(tpp)$_2$]	25.6	8

[a]This work.

The progress of the reaction was also monitored by ^{1}H NMR spectroscopy. Figure 8 demonstrates the ^{1}H NMR spectra of ylide, styrene, iodoether, dihydrofuran, and the reaction mixture catalyzed by complex **2** (0.5 mg of catalyst; reaction time 45 s). The resonance signals observed at 1.05 ppm in the spectra of iodoether and at 1.14 ppm in the spectra of dihydrofuran are attributed to the methyl group protons, respectively. The presence of both signals, slightly shifted to 1.07 and 1.16 ppm, in the spectra of the reaction mixture is an indication of iodoether and dihydrofuran formation.

Figure 9 shows the LC−ESI-MS spectrum of the reaction mixture catalyzed by **2** (4.0 mg of catalyst; reaction time 120 s). The chromatograph shows that the reaction mixture contains both dihydrofuran and iodoether attributed to the fragments at m/z 242.9 and 342.9, respectively (Figures S21−S29 in the SI).

Because the reaction of phenyliodonium dimedonate with styrene under irradiation for 1 h led to the formation of dihydrofuran (reaction 1), we have studied the synergistic effect of the catalysts **1**−**5** and UVC radiation in a photocatalytic experiment. Phenyliodonium dimedonate with styrene in dichloromethane reacted under UVC radiation under a low-pressure (15 W) mercury lamp (germicidal; λ_{max} = 254 nm) at room temperature, in the presence of catalysts **1**−**5**. The progress of the reaction was monitored by ^{1}H NMR (Figure S30 in the SI). The dihydrofuran/iodoether ratio was determined by integration of the signals at 1.16 and at 1.07 ppm, respectively [dihydrofuran/iodoether: 1.2/1 (**1**), 1.6/1 (**2**), 1.4/1 (**3**), 1.8/1 (**4**), and 1.5/1 (**5**)]. The order of the photocatalytic activity followed was **4** > **2** > **5** > **3** > **1**. Therefore, under these conditions, the tetrahedral compound **4** demonstrated the higher effect. However, the higher dihydrofuran/iodoether ratio was achieved when the reaction mixture was treated by **2** through heating for 45 s. The differences in the catalytic activity among tetrahedral and linear complexes in the case of photocatalysis should be attributed to their different photosensitivities. The photosensitivity of the catalysts was measured from their UV spectra in a 2.5 × 10^{-5} M solution under irradiation periods of 0, 15, 30, and 45 s (Figures S31 and S32 in the SI). The ΔC ($\Delta C = \Delta A/\varepsilon$) values, determined at the wavelength of the maximum ΔA, are as follows: **1**, 2.0 × 10^{-5} (286 nm); **2**, 1.3 × 10^{-5} (283 nm); **3**, 1.6 × 10^{-5} (266 nm); **4**,

dx.doi.org/10.1021/ic500727z | Inorg. Chem. XXXX, XXX, XXX−XXX

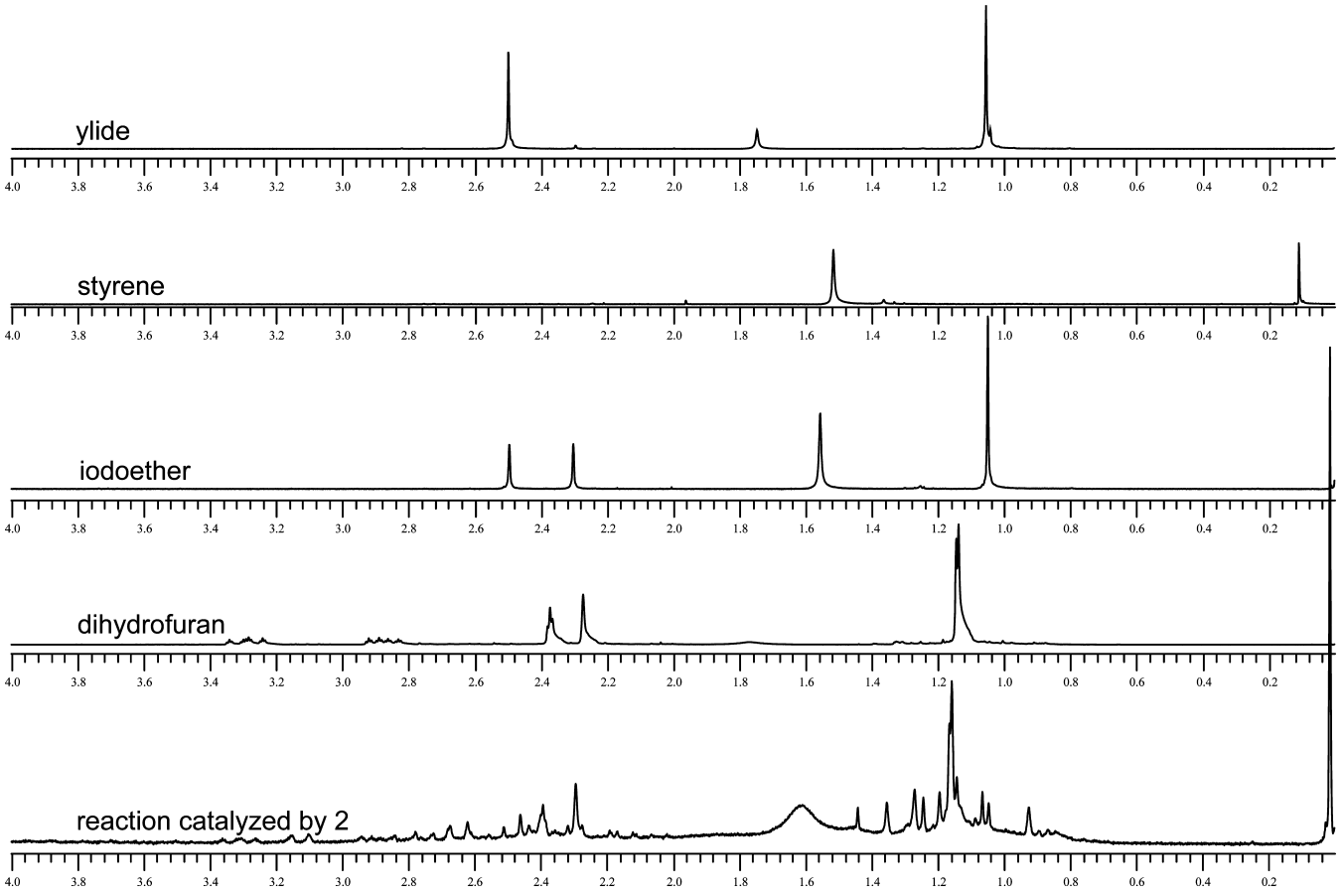

Figure 8. ^{1}H NMR spectra of ylide, styrene, iodoether, benzo[*b*]furan, and the reaction mixture catalyzed by **2** (0.5 mg of catalyst; reaction time 45 s).

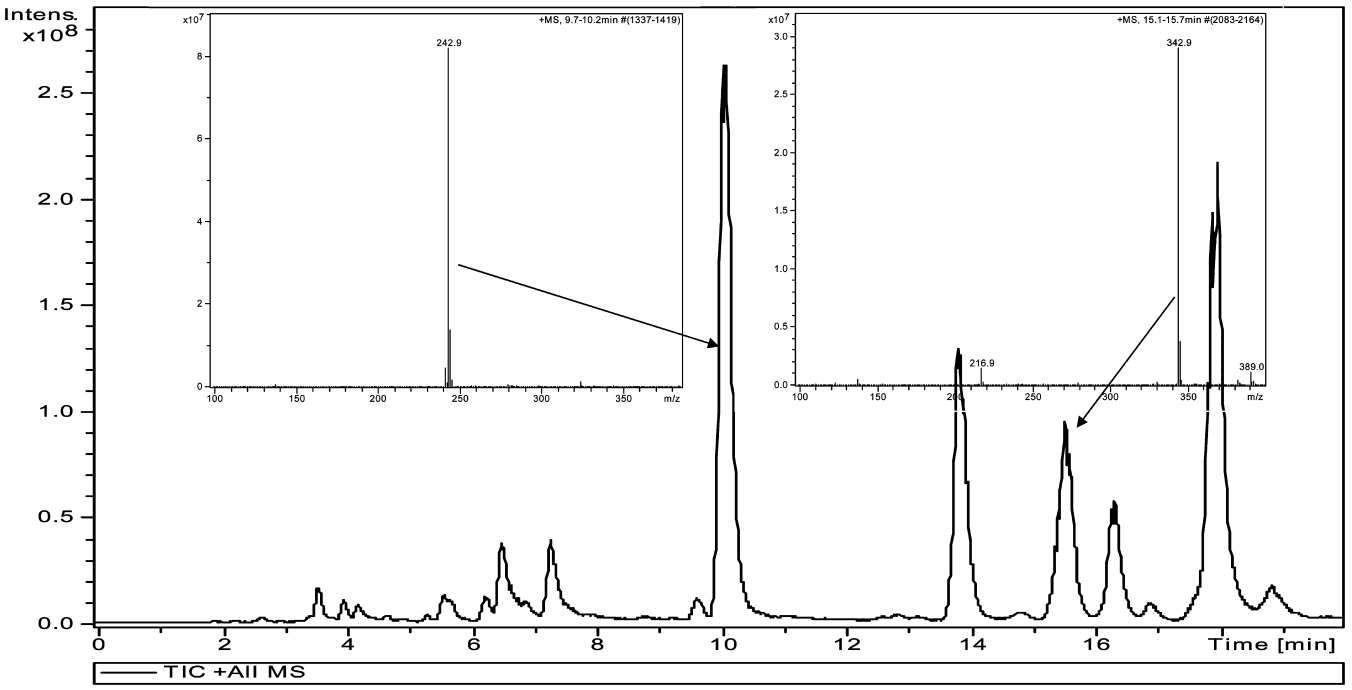

Figure 9. LC–ESI-MS spectrum of the reaction mixture catalyzed by **2** (4.0 mg of catalyst; reaction time 120 s).

1.5×10^{-5} (259 nm); **5**, 1.7×10^{-5} (253 nm). Thus, the order of the photosensitivity of the catalyst is **2** > **4** > **3** > **5** > **1**. Because the photocatalytic activity followed a similar order (**4** > **2** > **5** > **3** > **1**), it can be concluded that the lower photosensitivity of the catalyst led to the higher dihydrofuran/iodoether ratio.

Computational Studies. The higher catalytic activity of the dimeric linear complexes (**1** and **2**) in contrast to the

dx.doi.org/10.1021/ic500727z | *Inorg. Chem.* XXXX, XXX, XXX–XXX

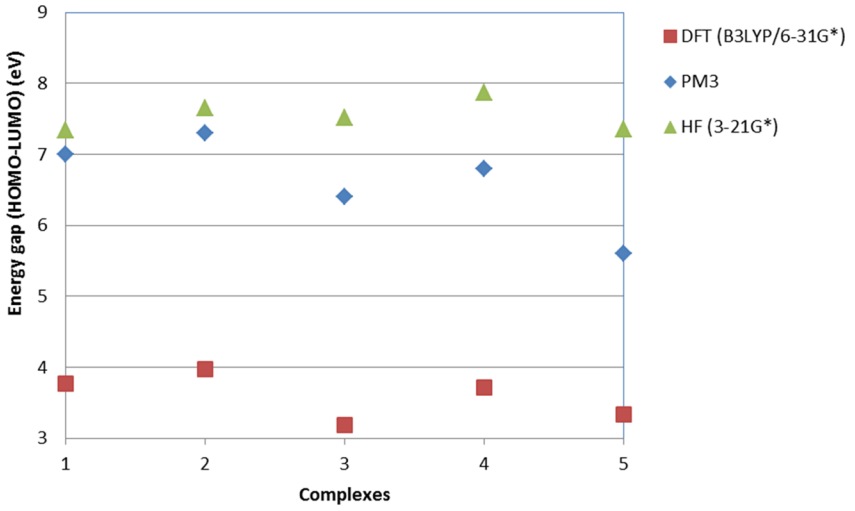

Figure 10. Stability of copper(II) complexes measured by the HOMO−LUMO gap energy.

monomeric tetrahedral ones (**3**−**5**) and the reverse relation between the catalytic activity and photosensitivity prompted us to perform theoretical calculations. Experiments showed that the nuclearity of the complexes plays a major role for the catalysis and complexes **1** and **2** demonstrate stronger catalytic activity than complexes **3**−**5**. A parameter that possibly significantly affects this issue is the stability of the complexes, which is successfully probed by the highest occupied minus the lowest unoccupied molecular level Δ(HOMO − LUMO) energy gap. Figure 10 shows the corresponding values for all complexes under three different levels of theory. There is a remarkable resemblance between semiempirical PM3 and DFT (B3LYP/6-31G*) methods regarding the stability trend, which, however, is normally not accompanied by similar absolute values. Previous studies[16] have shown the applicability of DFT(B3LYP/6-31G*) (DFT = density functional theory) calculations on these systems, while other studies have proved that the combination of PM3 and DFT(B3LYP/6-31G*) can successfully predict the molecular properties of copper(II) complexes.[17] Our results showed that the increased chemical stability of **1** and **2** probably increases their catalytic activity compared to **3**−**5**. The catalyst stability calculated by the mean of DFT theory [Δ(HOMO − LUMO)] follows the order **2** > **1**> **4** > **5** > **3** (Figure 10), which is identical with the catalytic activity order found experimentally (**2** > **1** > **4** = **5** > **3**), supporting further our assumption about the relationship between the catalyst stability and activity (see the photocatalytic activity). Our findings with the HF/3-21G* method are contradictory to both the experimental and the rest of the theoretical results, and therefore we conclude that they are not capable of describing such systems.

CONCLUSIONS

Dihydrofurans and their derivatives have demonstrated a wide range of applications in modern pharmaceutical research, and the development of novel synthetic routes for cases such as the reaction of phenyliodonium dimedonate with styrene (Scheme 1) has been investigated since the late 1980s.[6] The present study aims at the development of new complexes with high catalytic efficiency for the production of dihydrofurans. Five new mixed-ligand copper(I) halide complexes with TUC (**1**), MTUC (**2**, **4**, and **5**), and MPMTH (**3**) and tpp with tetrahedral geometry around the metal center were prepared and characterized. Complexes **1** and **2** are dimers with tetrahedral geometry around the metal center. The nature of the Cu1−S1−Cu2 bond leads to a linear configuration. Because of the orientation of the keto and/or methyl groups of TUC and MTUC (Scheme 1), only one stereoisomer was isolated. This orientation is dictated by deprotonation of the nitrogen atom (Scheme 1) and the intramolecular N[H]···Cl hydrogen-bonding interactions (Scheme 1). Complexes **3**−**5** are monomers with slightly distorted tetrahedral geometry because of the arrangement of bulky tpp ligands. Only one stereoisomer has also been obtained because of the orientation of the keto and/or methyl groups of MPMTH and MTUC in the cases of **3**−**5** (Scheme 1). Intramolecular hydrogen-bonding interactions between the H[N] and halogen atoms (Scheme 1) result in the formation of the one isomer. In the case of **5**, strong intramolecular hydrogen-bonding interactions H6[N6]···O3 = 2.01(2) Å lead to dimerization, further stabilizing the conformation (Figure 7).

The catalytic activity of the copper(I) complexes toward the formation of dihydrofurans from phenyliodonium dimedonate and styrene has shown that the mechanism might not be a redox process because copper(II) acetate[6] also catalyzes the same reaction. The copper(I) complexes tested were stable in solution. Computational studies have shown that the increased chemical stability of **1** and **2** correlates well with their catalytic activity by remaining active over longer periods compared to **3**−**5**. Complexes of TUC and its methyl (MTU) or propyl (PTU) derivatives exhibit higher catalytic activity, which is also observed for tbSb in the case of the dimeric complex of copper(I) iodide with tbSb. The presence of the iodide in the coordination sphere increases the activity, but the linear binuclear copper chloride complexes **1** and **2** exert the highest catalytic activity up to now (Table 4). The synergistic effect of triarylphsphine is observed by the decreasing activity upon going from the mixed-lignad complexes [CuI(tptp)$_2$(ptu)] and [CuI(tpp)$_2$(ptu)] to [CuI(ptu)$_2$](toluene). Dimeric copper(I) complexes **1** and **2** and [(tpSb)$_2$Cu(μ_2-I)$_2$Cu(tpSb)$_2$] demonstrate higher catalytic activity than the monomer ones, although the binuclear complexes [(tpp)Cu(μ_2-I)$_2$Cu(tpp)$_2$] and [(tpp)-Cu(μ_2-Cl)$_2$Cu(tpp)$_2$] exhibit lower activity, which migth be attributed to the absence of thionucleotide and additionally by the presence of a chloride anion instead of iodide in the coordination sphere. It is therefore concluded that the nuclearity

dx.doi.org/10.1021/ic500727z | Inorg. Chem. XXXX, XXX, XXX−XXX

Table 5. Structure Refinement Details for Complexes 1−5

	1	2	3	4a	4b	5
empirical formula	$C_{76}H_{63}ClCu_2N_2OP_4S$	$C_{77}H_{65}ClCu_2N_2OP_4S$	$(C_{41}H_{36}ClCuN_2P_2S)\cdot{}^1/_2CH_3OH$	$C_{41}H_{36}CuBrN_2OP_2S$	$C_{41}H_{36}CuBrN_2OP_2S$	$2(C_{41}H_{36}CuIN_2OP_2S)\cdot CH_3CN$
fw	1338.75	1352.78	765.73	810.17	810.17	1755.39
T (K)	295	295(2)	100(1)	−100(1)	295(2)	180(2)
cryst syst	triclinic	triclinic	monoclinic	monoclinic	triclinic	monoclinic
space group	$P\bar{1}$	$P\bar{1}$	$P2_1/c$	$C2/c$	$P\bar{1}$	$C2/c$
a (Å)	13.096(3)	13.243(3)	14.753(3)	24.766(4)	10.730(2)	24.7689(13)
b (Å)	13.828(3)	13.812(3)	10.024(2)	10.940(2)	13.968(2)	10.8836(7)
c (Å)	21.647(4)	21.616 (5)	24.711(3)	54.536(6)	26,324(5)	29.4008(17)
α (deg)	98.08(3)	97.44(2)	90	90	87.73(2)	90
β (deg)	101.93(2)	101.59(3)	91.78(2)	91.85(2)	82.98(3)	95.273(4)
γ (deg)	113.53(3)	114.01(3)	90	90	75.88(2)	90
V (Å^3)	3406.0(17)	3438.1(18)	3652.6(11)	14768(4)	3797.13(12)	7892.2(8)
Z	2	2	4	16	4	4
F(000)	1384	1400	1588	6624	1656	3532
ρ_{calcd} (g cm^{-3})	1.31	1.31	1.39	1.46	1.42	1.497
μ (mm^{-1})	0.83	2.63	0.85	1.85	1.80	1.5
θ range	2.76−25.0 0	3.61−70.00	2.94−25.00	2.82−25.00	2.79−28.25	2.05−26.72
data collected, unique (R_{int})	38814, 12021 (0.094)	24166, 12751 (0.044)	15272, 6416 (0.052)	27805, 12943 (0.093)	30050, 15737 (0.062)	17130, 8100 (0.022)
obsd reflns [$I > 2\sigma(I)$]	6658	9964	5033	10179	9321	6331
R1, wR2 [$I > 2\sigma(I)$], S	0.057, 0.121 0.92	0.04391, 0.1243, 1.11	0.0435, 0.0891, 1.07	0.157, 0.287, 2.46	0.0482,0.0920, 1.01	0.0287, 0.0725, 1.04
max/min $\Delta\rho$ (e Å^{-3})	0.63/−0.36	0.49/−0.49	0.47/−0.45	2.83/−1.65	0.67/−0.64	0.57/−0.53

and type of ligand have a strong effect on the complexes' catalytic activity.

EXPERIMENTAL SECTION

Materials and Instruments. All solvents used were reagent grade. Copper(I) halides (Riedel deHaen), 2-thiouacil (TUC; Fluka Chemica), 6-methyl-2-thiouacil (MTUC; Aldrich), 4-methyl-2-mercaptopyrimidine·HCl (MPMTH; Aldrich), and triphenylphosphine (tpp; Merck) were used with no other purification prior to use (exception: MPMTH·HCl was treated with an equimolar amount of NaOH in MeOH). Melting points were measured in open tubes with a Stuart scientific apparatus and are uncorrected. IR spectra in the region of 4000−370 cm^{-1} were obtained in KBr disks with a PerkinElmer Spectrum GX FT-IR spectrometer. A Jasco UV−vis−NIR spectrometer was used to obtain the electronic absorption spectra.

Synthesis and Crystallization of $[Cu_2(tpp)_4(TUC)Cl]$ (1), $[Cu_2(tpp)_4(MTUC)Cl]$ (2), $[Cu(tpp)_2(MPMTH)Cl]\cdot 2CH_3OH$ (3), $[Cu(tpp)_2(MTUC)Br]$ (4), and $[Cu(tpp)_2(MTUC)I]$ (5). Complexes **1** and **2** were prepared as follows: 0.50 mmol of CuCl (0.05 g), 1.00 mmol of tpp (0.26 g), and 0.50 mmol (0.06 g) of TUC (**1**) or 0.50 mmol (0.07 g) of MTUC (**2**) were suspended in 20 cm^3 of a methanol/acetonitrile solution (1:1). In the case of **1**, 2 cm^3 of dimethylformamide was also added. The suspensions were stirred and heated under reflux. Clear solutions were formed after a period of 4−5 h. The solutions were filtered off, and they were kept in darkness at room temperatures. A few days later, colorless crystals suitable for single-crystal analysis by X-ray crystallography were grown and collected by filtration. Complexes **3**−**5** were prepared as follows: 0.50 mmol(0.05 g) of CuCl (**3**), 0.50 mmol (0.07 g) of CuBr (**4**), 0.50 mmol (0.10 g) of CuI (**5**), 1.00 mmol (0.26 g) of tpp, and 0.50 mmol (0.08 g) of MPMTH·HCl (**3**) or 0.50 mmol (0.07 g) of MTUC (**4** and **5**) were suspended in 20 cm^3 of a methanol/acetonitrile solution (1:1). The suspensions were stirred under reflux. After 4−5 h, clear solutions were formed. The solutions were then filtered off, and they were kept in darkness at room temperatures. Orange (**3**) and colorless (**4** and **5**) crystals suitable for single-crystal analysis by X-ray crystallography were grown and collected.

1. White crystals. Yield: 0.05 g (7%). Mp: 205−209 °C. Elem anal. Calcd for $C_{76}H_{63}ClCu_2N_2OP_4S$: C, 68.18; H, 4.74; N, 2.09; S, 2.39. Found: C, 67.70; H, 4.86; N, 2.32; S, 2.21. IR cm^{-1} (KBr): 3444w, 3046s, 1647s, 1531vs, 1432vs, 1282vs, 1093s, 744vs, 695vs, 513s. ^{1}H NMR ($CDCl_3$, ppm): 7.4−7.1 (multi, $H_{aromatic}$), 5.7 (singlet, H(C) from pyrimide ring). UV−vis [CH_2CH_2; λ, nm (log ε, M^{-1} cm^{-1})]: 231 (4.61), 262 (4.35) (Figures S6, S15, and S31 in the SI).

2. White crystals. Yield: 0.16 g (24%). Mp: 209−214 °C. Elem anal. Calcd for $C_{77}H_{65}ClCu_2N_2OP_4S$: C, 68.36; H, 4.84; N, 2.07; S, 2.37. Found: C, 68.55; H, 4.63; N, 1.94; S, 2.60. IR cm^{-1} (KBr): 3050w, 1648vs, 1607vs, 1534vs, 1433vs, 1094s, 745vs, 695vs, 513vs. ^{1}H NMR ($CDCl_3$, ppm): 7.5−7.2 (multi, $H_{aromatic}$), 5.6 (singlet, H(C) from pyrimide ring), 2.1 (singlet H(C) from methyl group), 2.0 (singlet H(N) from amide group). UV−vis [CH_2CH_2; λ, nm (log ε, M^{-1} cm^{-1})]: 231 (4.60), 272 (4.35) (Figures S7, S16, and S31, M^{-1} cm^{-1}).

3. orange crystals. Yield: 0.11 g (30%). Mp: 186−187 °C. Elem anal. Calcd for $C_{41}H_{36}ClCuN_2P_2S\cdot{}^1/_2CH_3OH$: C, 65.09; H, 5.00; N, 3.66; S, 4.19. Found: C, 65.25; H, 4.92; N, 3.78; S, 4.40. IR cm^{-1} (KBr): 3423w, 3050s, 1611s, 1564vs, 1475s, 1245s, 1179s, 745vs, 697vs, 510s. ^{1}H NMR ($CDCl_3$, ppm): 7.5−7.2 (multi, $H_{aromatic}$), 6.5 (singlet, H(C) from pyrimide ring), 2.4 (singlet H(C) from methyl group), 2.0 (singlet H(N) from amide group). UV−vis [CH_2CH_2; λ, nm (log ε, M^{-1} cm^{-1})]: 231 (4.34), 266 (4.29) (Figures S8, S17, and S31 in the SI).

4. White crystals. Yield: 0.14 g (34%). Mp: 194−196 °C. Elem anal. Calcd for $C_{41}H_{36}CuBrN_2OP_2S$: C, 60.78; H, 4.47; N, 3.46; S, 3.96. Found: C, 61.25; H, 4.64; N, 3.87; S, 4.57. IR cm^{-1} (KBr): 3050w, 1650s, 1529vs, 1434vs, 1267s, 1193s, 1094s, 746s, 694s, 513s. ^{1}H NMR ($CDCl_3$, ppm): 7.5−7.2 (multi, $H_{aromatic}$), 5.6 (singlet, H(C) from pyrimide ring), 2.1 (singlet H(C) from methyl group), 2.0 (singlet H(N) from amide group). UV−vis [CH_2CH_2; λ, nm (log ε, M^{-1} cm^{-1})]: 231 (4.38), 268 (4.21) (Figures S9, S18, and S31 in the SI).

5. White crystals. Yield: 0.21 g (48%). Mp: 185−188 °C. Elem anal. Calcd for $2(C_{41}H_{36}CuIN_2OP_2S)\cdot CH_3CN$: C, 57.48; H, 4.30; N, 3.99; S, 3.65. Found: C, 57.90; H, 4.28; N, 3.67; S, 3.46. IR cm^{-1} (KBr): 3053w, 1637vs, 1540vs, 1434s, 1348s, 1167s, 841s, 743s, 694s, 513s. ^{1}H NMR ($CDCl_3$, ppm): 7.7−7.2 (multi, $H_{aromatic}$), 5.6 (singlet, H(C) from pyrimide ring), 2.2 (singlet H(C) from methyl group), 2.0 (singlet H(N) from amide group). UV−vis [CH_2CH_2; λ, nm (log ε, M^{-1} cm^{-1})]: 231 (4.49), 263 (4.21) (Figures S10, S19, and S31 in the SI).

X-ray Structure Determination. Diffraction data for the complexes were collected by ω scan for **1** and **4b** at room temperature and for **3** and **4a** at 100(1) K on an Agilent Technologies XCalibur diffractometer (Eos detector) with graphite-monochromated Mo Kα radiation (λ = 0.71073 Å), for **2** at room temperature on an Agilent Technologies SuperNova diffractometer (Atlas detector) with

dx.doi.org/10.1021/ic500727z | Inorg. Chem. XXXX, XXX, XXX−XXX

mirror-monochromatized Cu Kα radiation (λ = 1.54178 Å), and for **5** on a STOE IPDS 2 diffractometer with graphite-monochromatized Mo Kα radiation (λ = 0.71073 Å). The data were corrected for Lorentz polarization and absorption effects.[18a] For **4**, because of the very long unit-cell parameter, the detector was moved away from the source; in general, this data was of lower quality, however allowing reasonable structure analysis. Accurate unit-cell parameters were determined by a least-squares fit of reflections of highest intensity, chosen from the whole experiment [8623 (**1**), 9838 (**2**), 4961 (**3**), 9918 (**4a**), 5329 (**4b**), and 12136 (**5**)] . The structures were solved with *SIR92*[18b] and refined with the full-matrix least-squares procedure on F^2 by *SHELXL-2013*;[18c] most of the calculations were performed within the *WinGX* program suite.[18d] Scattering factors incorporated in *SHELXL-2013* were used. All non-hydrogen atoms were refined anisotropically, and hydrogen atoms were placed in the calculated positions and refined as "riding model" with the isotropic displacement parameters set at 1.2 (1.5 for methyl groups) times the U_{eq} value for the appropriate non-hydrogen atom. Only in the structure of **5**, hydrogen atoms involved in hydrogen bonds were located in the difference Fourier maps, and their positions were refined. In one of the symmetry-independent molecules of structure **4b**, phenyl rings in one of the PPh_3 groups are disordered over two alternative positions. Weak constraints were applied to the geometry and displacement parameters of the disordered atoms. Similar restraints were also used in the refinement of structure **4a**; the crystals were of low quality, but the final results allow for structure analysis. In turn, in structure **5**, a disordered solvent/acetonitrile molecule was found, the non-hydrogen atoms of this molecule were refined isotropically, and no attempts were performed to locate the positions of the hydrogen atoms of its methyl group. Relevant crystal data are listed in Table 5, together with refinement details.

Supplementary data for complexes **1**−**5** are available from the Cambridge Crystallographic Data Centre, 12 Union Road, Cambridge CB2 1EZ, U.K. (e-mail: deposit@ccdc.cam.ac.uk), upon request, quoting the deposition numbers CCDC 986656 (**1**), 986655 (**2**), 990782 (**3**), 990783 (**4a**), 990784 (**4b**), and 987589 (**5**).

Catalysis. In an Erlenmeyer spherical flask, the proper amounts of ylide, styrene, and catalyst are added. The reaction mixture is heated under continuous stirring to 110 °C. A few seconds later (45 or 120 s), the solid ylide turned into a clear orange or dark liquid. Dihydrofuran yield was detected by the means of HPLC.

HPLC Assay. The sample constituents were isocratically separated using acetonitrile/water (55/45) with a flow rate of 1 mL min^{-1}, using a chromatographic system comprised of a Shimadzu liquid chromatograph equipped with two LC-8A solvent delivery pumps coupled to a communication bus module (CBM-20A), which was used to control sample injection (SIL-10AP autosampler). The peaks representing the sample constituents were recognized by both their retention time and spectral pattern recorded on a Shimadzu SPD-M20A diode array detector working under *LC Solution v.1.2.3* chromatography software.

Computational Details. All calculations were carried out using the *SPARTAN '08* software package.[19] The equilibrium gas-phase structures were first fully optimized with the PM3 semiempirical method. In all cases, the energy minima at the found stationary points were checked by constructing the Hessian matrix. Positive eigenvalues were found for complexes **3**−**5** without imposing any geometry constraints, while for **1** and **2**, we kept the distance of the Cu−S bond fixed to the values received by X-ray diffraction analysis. PM3 optimization reliably calculated the geometric parameters of the structures. Semiempirical calculations were followed by single-point-energy calculations carried out at the DFT(B3LYP/6-31G*) and HF/3-21G* levels.

■ ASSOCIATED CONTENT

Supporting Information

X-ray crystallographic data in CIF format and ^{1}H NMR, IR, ESI-MS, and UV spectra. This material is available free of charge via the Internet at http://pubs.acs.org.

■ AUTHOR INFORMATION

Corresponding Author

*E-mail: shadjika@uoi.gr. Tel.: 30-26510-08374.

Notes

The authors declare no competing financial interest.

■ ACKNOWLEDGMENTS

This research was carried out in partial fulfillment of the requirements for the Master thesis of D.C.C. within the graduate program of the Chemistry Department, at the University of Ioannina, Ioannina, Greece, under the supervision of S.K.H. A.O. is a scholar of the project "Scholarship support for Ph.D. students specializing in majors strategic for Wielkopolska's development", submeasure 8.2.2 Human Capital Operational Programme, cofinanced by the European Union under the European Social Fund. A.O. was also supported by the Adam Mickiewicz Foundation during the academic year 2013−2014, which is acknowledged.

■ REFERENCES

(1) (a) Choi, H.-D.; Seo, P.-J.; Son, B.-W.; Kang, B. W. *Arch. Pharm. Res.* **2004**, *27*, 19−24. (b) Coy, E.-D.; Cuca, L.-E.; Sefkow, M. *Bioorg. Med. Chem. Lett.* **2009**, *19*, 6922−6925. (c) Venkatesan, A. M.; Dos Santos, O.; Ellingboe, J.; Evrard, D. A.; Harrison, B. L.; Smith, D. L.; Scerni, R.; Hornby, G. A.; Schechter, L. E.; Andree, T. H. *Bioorg. Med. Chem. Lett.* **2010**, *20*, 824−827.

(2) Connor, D. T.; Cetenko, W. A.; Mullican, M. D.; Sorenson, R. J.; Unangst, P. C.; Weikort, R. J.; Adolphson, R. L.; Kennedy, J. A.; Thueson, D. O.; Wright, J. C. D.; Conroyt, M. C. J. *J. Med. Chem.* **1992**, *35*, 958−965.

(3) Galal, S. A.; Abd El-All, A. S.; Abdallah, M. M.; El-Diwani, H. I. *Bioorg. Med. Chem. Lett.* **2009**, *19*, 2420−2428.

(4) Rida, S. M.; El-Hawassh, S. A.; Fahmy, H. T. Y.; Hazza, A. A.; El-Mellgy, M. M. M. *Arch. Pharm. Res.* **2006**, *29*, 826−833.

(5) Rizzo, S.; Riviere, C.; Piazzi, L.; Bisi, A.; Gobbi, S.; Bartolini, M.; Andrisano, V.; Morroni, F.; Tarozzi, A.; Monti, J.-P.; Rampa, A. J. *Med. Chem.* **2008**, *51*, 2883−2886.

(6) Hadjiarapoglou, L. P. *Tetrahedron Lett.* **1987**, *28*, 4449−4450.

(7) (a) Bakalbassis, E. G.; Spyroudis, S.; Tsipis, C. A. *Eur. J. Org. Chem.* **2008**, 1783−1788. (b) Kefalidis, C. E.; Kanakis, A. A.; Gallos, J. K.; Tsipis, C. A. *J. Organomet. Chem.* **2010**, *695*, 2030−2038.

(8) Paizanos, K.; Charalampou, D.; Kourkoumelis, N.; Kalpogiannaki, D.; Hadjiarapoglou, L. P.; Spanopoulou, A.; Lazarou, K.; Manos, M. J.; Tasiopoulos, A. J.; Kubicki, M.; Hadjikakou, S. K. *Inorg. Chem.* **2012**, *51*, 1248−12259.

(9) (a) Boyer, A.; Isono, N.; Lackner, S.; Lautens, M. *Tetrahedron* **2010**, *66*, 6468−6482. (b) Yong, K.; Salim, M.; Capretta, A. *J. Org. Chem.* **1998**, *63*, 9828−9833. (c) Succaw, G. L.; Doxsee, K. M. *Educ. Quim.* **2009**, 433−440. (d) Colobert, F.; Castanet, A.-C.; Abillard, O. *Eur. J. Org. Chem.* **2005**, 3334−3341. (e) Cacchi, S.; Fabrizi, G.; Goggiamani, A. *Org. Biomol. Chem.* **2011**, *9*, 641−652. (f) Stephen, A.; Hashmi, K.; Yang, W.; Rominger, F. *Angew. Chem., Int. Ed.* **2011**, *50*, 5762−5765. (g) Geary, W. J. *Coord. Chem. Rev.* **1971**, *7*, 81−122.

(10) (a) Palafox, M. A.; Rastogi, V. K.; Tanwar, R. P.; Mittal, L. *Spectrochim. Acta, Part A* **2003**, *59*, 2473−2486. (b) Grosmuire, L.; Delabre, J.-L. *J. Mol. Struct.* **2012**, *1011*, 42−49.

(11) (a) Gunasekaran, N.; Ng, S. W.; Tiekink, E. R. T.; Karvembu, R. *Polyhedron* **2012**, *34*, 41. (b) Shakhatreh, S.; Lalia-Kantouri, M.; Gdaniec, M.; Akrivos, P. D. *J. Coord. Chem.* **2012**, *65*, 251. (c) Lobana, T. S.; Kumari, P.; Kaur, I.; Kaur, N.; Garg, G.; Butcher, R. J. *J. Coord. Chem.* **2012**, *65*, 1750. (d) Aslanidis, P.; Cox, P. J.; Tsipis, A. C. *Dalton Trans.* **2010**, *39*, 10238. (e) Lobana, T. S.; Sharma, R.; Castinieras, A.; Butcher, R. J. *Z. Anorg. Allg. Chem.* **2010**, *636*, 2698. (f) Lao, L.; Pakawatchai, C.; Saithong, S.; Skelton, B. W. *Acta Crystallogr., Sect. E: Struct. Rep. Online* **2009**, *65*, m926. (g) Ghassemzadeh, M.; Tabatabaee, M.; Soleimani, S.; Neumuller, B. *Z. Anorg. Allg. Chem.*

2005, *631*, 1871. (h) Ferrari, M. B.; Bonardi, A.; Fava, G. G.; Pelizzi, C.; Tarasconi, P. *Inorg. Chim. Acta* **1994**, *223*, 77. (i) Ghassemzadeh, M.; Adhami, F.; Heravi, M. M.; Taeb, A.; Chitsaz, S.; Neumuller, B. *Z. Anorg. Allg. Chem.* **2002**, *628*, 2887. (j) Li, D.; Shi, W.-J.; Wu, T.; Ng, S. W. *Acta Crystallogr., Sect. E: Struct. Rep. Online* **2004**, *60*, m776.

(12) (a) Lobana, T. S.; Kaur, P.; Castineiras, A.; Turner, P.; Failes, T. W. *Struct. Chem.* **2008**, *19*, 727. (b) Sanghamitra, N. J. M.; Adwankar, M. K.; Juvekar, A. S.; Khurajjam, V.; Wycliff, C.; Samuelson, A. G. *Indian J. Chem., Sect. A: Inorg., Bio-inorg., Phys., Theor. Anal. Chem.* **2011**, *50*, 465. (c) Batsala, G. K.; Dokorou, V.; Kourkoumelis, N.; Manos, M. J.; Tasiopoulos, A. J.; Mavromoustakos, T.; Simic, M.; Golic-Grdadoinik, S.; Hadjikakou, S. K. *Inorg. Chim. Acta* **2012**, *382*, 146. (d) Lobana, T. S.; Rekha; Pannu, A. P. S.; Hundal, G.; Butcher, R. J.; Castineiras, A. *Polyhedron* **2007**, *26*, 2621. (e) Aslanidis, P.; Cox, P. J.; Divanidis, S.; Tsipis, A. C. *Inorg. Chem.* **2002**, *41*, 6875. (f) Ghassemzadeh, M.; Tabatabaee, M.; Pooramini, M. M.; Heravi, M. M.; Eslami, A.; Neumuller, B. *Z. Anorg. Allg. Chem.* **2006**, *632*, 786. (g) Lobana, T. S.; Sharma, R.; Sharma, R. *J. Coord. Chem.* **2009**, *62*, 1468. (h) Ghassemzadeh, M.; Heravi, M. M.; Fallahnedjad, L.; Neumuller, B. *Z. Anorg. Allg. Chem.* **2008**, *634*, 352. (i) Tabatabaee, M.; Ghassemzadeh, M.; Sadeghi, A.; Shahriary, M.; Neumuller, B.; Rothenberger, A. *Z. Anorg. Allg. Chem.* **2009**, *635*, 120. (j) Ghassemzadeh, M.; Adhami, F.; Heravi, M. M.; Taeb, A.; Chitsaz, S.; Neumuller, B. *Z. Anorg. Allg. Chem.* **2001**, *627*, 815.

(13) (a) Lobana, T. S.; Khanna, S.; Hundal, G.; Butcher, R. J.; Castineiras, A. *Polyhedron* **2009**, *28*, 3899. (b) Gunasekaran, N.; Ramesh, P.; Ponnuswamy, M. N. G.; Karvembu, R. *Dalton Trans.* **2011**, *40*, 12519. (c) Lobana, T. S.; Khanna, S.; Hundal, G.; Kaur, P.; Thakur, B.; Attri, S.; Butcher, R. J. *Polyhedron* **2009**, *28*, 1583. (d) Lobana, T. S.; Rekha; Butcher, R. J.; Castineiras, A.; Bermejo, E.; Bharatam, P. V. *Inorg. Chem.* **2006**, *45*, 1535. (e) Ferrari, M. B.; Fava, G. G.; Lanfranchi, M.; Pelizzi, C.; Tarasconi, P. *Inorg. Chim. Acta* **1991**, *181*, 253. (f) Skoulika, S.; Aubry, A.; Karagianidis, P.; Aslanidis, P.; Papastefanou, S. *Inorg. Chim. Acta* **1991**, *183*, 207. (g) Lobana, T. S.; Khanna, S.; Butcher, R. J.; Hunter, A. D.; Zeller, M. *Polyhedron* **2006**, *25*, 2755. (h) Singh, R.; Dikshit, S. K. *Polyhedron* **1995**, *14*, 1799. (i) Aslanidis, P.; Kyritsis, S.; Lalia-Kantouri, M.; Wicher, B.; Gdaniec, M. *Polyhedron* **2012**, *48*, 140. (j) Wani, K.; Pakawatchai, C.; Saithong, S. *Acta Crystallogr., Sect. E: Struct. Rep. Online* **2013**, *69*, m34.

(14) (a) Shakhatreh, S.; Lalia-Kantouri, M.; Gdaniec, M.; Akrivos, P. D. *J. Coord. Chem.* **2012**, *65*, 251. (b) Kaltzoglou, A.; Cox, P. J.; Aslanidis, P. *Inorg. Chim. Acta* **2005**, *358*, 3048. (c) Aslanidis, P.; Cox, P. J.; Divanidis, S.; Karagiannidis, P. *Inorg. Chim. Acta* **2004**, *357*, 1063. (d) Lobana, T. S.; Rekha; Sidhu, B. S.; Castineiras, A.; Bermejo, E.; Nishioka, T. *J. Coord. Chem.* **2005**, *58*, 803. (e) Karagiannidis, P.; Aslanidis, P.; Papastefanou, S.; Mentzafos, D.; Hountas, A.; Terzis, A. *Polyhedron* **1990**, *9*, 981. (f) Lecomte, C.; Skoulika, S.; Aslanidis, P.; Karagiannidis, P.; Papastefanou, S. *Polyhedron* **1989**, *8*, 1103. (g) Lobana, T. S.; Khanna, S.; Butcher, R. J. *Z. Anorg. Allg. Chem.* **2007**, *633*, 1820. (h) Lobana, T. S.; Sultana, R.; Hundal, G. *Polyhedron* **2008**, *27*, 1008. (i) Cox, P. J.; Kaltzoglou, A.; Aslanidis, P. *Inorg. Chim. Acta* **2006**, *359*, 3183. (j) Aslanidis, P.; Cox, P. J.; Tsaliki, P. *Polyhedron* **2008**, *27*, 3029. (k) Singh, R.; Dikshit, S. K. *Acta Crystallogr., Sect. C: Cryst. Struct. Commun.* **1996**, *52*, 635.

(15) (a) Aslanidis, P.; Cox, P. J.; Karagiannidis, P.; Hadjikakou, S. K.; Antoniadis, C. D. *Eur. J. Inorg. Chem.* **2002**, 2216. (b) Aslanidis, P.; Hadjikakou, S. K.; Karagiannidis, P.; Gdaniec, M.; Kosturkiewicz, Z. *Polyhedron* **1993**, *12*, 2221. (c) Venkatraman, R.; Sitole, L.; Wilson, M. R.; Fronczek, F. R. *Acta Crystallogr., Sect. E: Struct. Rep. Online* **2006**, *62*, m2992. (d) Nimthong, R.; Pakawatchai, C.; Saithong, S.; Charmant, J. P. H. *Acta Crystallogr., Sect. E: Struct. Rep. Online* **2008**, *64*, m977. (e) Wattanakanjana, Y.; Pakawatchai, C.; Saithong, S.; Piboonphon, P.; Nimthong, R. *Acta Crystallogr., Sect. E: Struct. Rep. Online* **2012**, *68*, m1417. (f) Jiang, Y.-H.; Qiu, Q.-M.; Jiang, R.-X.; Huang, X.; Jin, Q.-H. *Acta Crystallogr., Sect. E: Struct. Rep. Online* **2012**, *68*, m1295. (g) Pakawatchai, C.; Wattanakanjana, Y.; Choto, P.; Nimthong, R. *Acta Crystallogr., Sect. E: Struct. Rep. Online* **2012**, *68*, m773.

(16) (a) Chachkov, D. V.; Mikhailov, O. V.; Russ, J. *Inorg. Chem.* **2009**, *54*, 1952−1956. (b) Alagona, G.; Ghio, C. *Phys. Chem. Chem. Phys.* **2009**, *11*, 776. (b) Fraile, J. M.; García, J. I.; Martínez-Merino, V.; Mayoral, J. A.; Salvatella, L. *J. Am. Chem. Soc.* **2001**, *123*, 7616−7625. (c) Fraile, J. M.; García, J. I.; Gil, M. J.; Martínez-Merino, V.; Mayoral, J. A.; Salvatella, L. *Chem.—Eur. J.* **2004**, *10*, 758−765.

(17) Wang, M.-Z.; Meng, Z.-X.; Liu, B.-L.; Cai, G.-L.; Zhang, C.-L.; Wang, X.-Y. *Inorg. Chem. Commun.* **2005**, *8*, 368−371.

(18) (a) *CrysAlis*^{Pro}; Agilent Technologies: Santa Clara, CA, 2012. (b) Altomare, A.; Cascarano, G.; Giacovazzo, C.; Guagliardi, A.; Burla, M. C.; Polidori, G.; Camalli, M. *J. Appl. Crystallogr.* **1994**, *27*, 435. (c) Sheldrick, G. M. *Acta Crystallogr.* **2008**, *A64*, 112−122. (d) Farrugia, L. J. *J. Appl. Crystallogr.* **2012**, *45*, 849−854.

(19) Molnar, L. F.; Jung, Y.; Kussmann, J.; Ochsenfeld, C.; Brown, S. T.; Gilbert, A. T. B.; Slipchenko, L. V.; Levchenko, S. V.; O'Neill, D. P.; DiStasio, R. A.; Lochan, R. C.; Wang, T.; Beran, G. J. O.; Besley, N. A.; Herbert, J. M.; Lin, C. Y.; Van Voorhis, T.; Chien, S. H.; Sodt, A.; Steele, R. P.; Rassolov, V. A.; Maslen, P. E.; Korambath, P. P.; Adamson, R. D.; Austin, B.; Baker, J.; Byrd, E. F. C.; Dachsel, H.; Doerksen, R. J.; Dreuw, A.; Dunietz, B. D.; Dutoi, A. D.; Furlani, T. R.; Gwaltney, S. R.; Heyden, A.; Hirata, S.; Hsu, C.-P.; Kedziora, G.; Khalliulin, R. Z.; Klunzinger, P.; Lee, A. M.; Lee, M. S.; Liang, W. Z.; Lotan, I.; Nair, N.; Peters, B.; Proynov, E. I.; Pieniazek, P. A.; Rhee, Y. M.; Ritchie, J.; Rosta, E.; Sherrill, C. D.; Simmonett, A. C.; Subotnik, J. E.; Woodcock, H. L., III; Zhang, W.; Bell, A. T.; Chakraborty, A. K.; Chipman, D. M.; Keil, F. J.; Warshel, A.; Hehre, W. J.; Schaefer, H. F.; Kong, J.; Krylov, A. I.; Gill, P. M. W.; Head-Gordon, M. *Phys. Chem. Chem. Phys.* **2006**, *8*, 3172.